Cell. Mol. Life Sci. 66 (2009) 1126 – 1134
1420-682X/09/061126-9
DOI 10.1007/s00018-009-8829-8

Cellular and Molecular Life Sciences

Research Article

Cathepsin X-mediated β_2 integrin activation results in nanotube outgrowth

N. Obermajer[a, †, *], Z. Jevnikar[a, †], B. Doljak[a], A. M. Sadaghiani[b], M. Bogyo[b] and J. Kos[a, c]

[a] Department of Pharmaceutical Biology, Faculty of Pharmacy, Aškerčeva 7, 1000 Ljubljana (Slovenia), Fax: +386-1-425-80-31, e-mail: natasa.obermajer@ffa.uni-lj.si
[b] Department of Pathology, Stanford University School of Medicine, 300 Pasteur Drive, Stanford, CA 94305 (USA)
[c] Department of Biotechnology, Jozef Stefan Institute, Jamova 39, 1000 Ljubljana (Slovenia)

Received 26 December 2008; received after revision 26 January 2009; accepted 27 January 2009
Online First 6 February 2009

Abstract. Membrane nanotubes were recently described as a new principle of cell–cell communication enabling complex and specific messaging to distant cells. Calcium fluxes, vesicles, and cell-surface components can all traffic between cells connected by nanotubes. Here we report for the first time the mechanism of membrane nanotube formation in T cells through LFA-1 (CD11a/CD18; $\alpha_L\beta_2$) integrin activation by the cysteine protease cathepsin X. Cathepsin X is shown to induce persistent LFA-1 activation. Cathepsin X-upregulated T cells exhibit increased homotypic aggregation and polarized, migration-associated morphology in 2D and 3D models, respectively. In these cells, extended uropods are frequently formed, which subsequently elongate to nanotubes connecting T lymphocytes. Our results demonstrate that LFA-1 activation with subsequent cytoskeletal reorganization induces signal transmission through a physically connected network of T lymphocytes for better coordination of their action at various stages of the immune response.

Keywords. Cathepsin X, nanotubes, uropod, integrin LFA-1, T lymphocytes.

Introduction

Membrane nanotubes comprise thin membranous channels mediating continuity between the plasma membranes of connected cells [1, 2]. They were first named tunneling nanotubes for the cellular interconnections formed by PC12 cells, with a diameter of 50–200 nm [1]. They exhibit diverse structural properties (thin nanotubes exhibit diameters of <0.7 μm; thick nanotubes exhibit diameters of >0.7 μm) [2] and the peculiar morphology raises the question of how they are generated. Actin reorganization has been consistently demonstrated to be essential for active protrusion and the importance of actin polymerization for nanotube formation has been reported by different groups [1, 3].

The local remodeling of actin is ultimately achieved by integrin recruitment. Integrins are membrane receptors binding either to counter-receptors on other cells or mediating interactions with components of the extracellular matrix [4]. The integrin lymphocyte function-associated antigen-1 (LFA-1; CD11a/CD18; $\alpha_L\beta_2$) is expressed on most leukocytes and plays a major role in regulating leukocyte polarization. Precise regulation of integrin activation occurs during

† These authors contributed equally to the present work.
* Corresponding author.

leukocyte adhesion and their directional migration [5].

We have shown that cysteine protease cathepsin X induces polarized migration-associated morphology in Jurkat T cells [6]. Cathepsin X is an important regulator of LFA-1 activity [7]. Cathepsin X-upregulated T lymphocytes exhibit increased LFA-1 activation, associated with increased homotypic cell-cell contact and cell cluster formation, and profound spontaneous development of cell polarization and uropod formation [6]. Although cathepsin X is a lysosomal protease, its localization and trafficking is dependent on the state of cell activation and, like some other lysosomal proteases [8], it is translocated towards the plasma membrane upon leukocyte activation [9, 10]. The mechanism of its translocation to the vicinity of integrin receptor is yet unclear; however its interaction with β_2 integrin subunit and LFA-1 integrin receptor activation was confirmed by immunoprecipitation and fluorescence resonance energy transfer (FRET) [7, 9].

In this study, the role of cathepsin X in nanotubes outgrowth was investigated. We show that cathepsin X-upregulated Jurkat T cells, exhibiting persistent LFA-1 integrin activation, are able to form cell contact-dependent and -independent membrane nanotubes. These nanotubes may transfer intracellular vesicles, such as lysosomes and mitochondria between distant Jurkat T cells and enable additional mechanism of cell-to-cell communication in the immune system.

Materials and methods

Cells. The $CD4^+$ T cell line Jurkat (from the American Type Culture Collection; ATCC; TIB-152) was cultured in RPMI 1640 (Sigma) supplemented with 5% FCS (HyClone), 2 mM L-glutamine (Sigma), 50 U/ml penicillin and 50 μg/ml streptomycin. Preparation of cathepsin X-upregulated Jurkat T cells is described in detail elsewhere [6]. Jurkat T lymphocytes were transfected with pcDNA3/cathepsin X vector using Lipofectamine 2000 (Invitrogen) and stable lines were selected in 400 μg/ml Geneticin (Gibco). Single cell clones were isolated by limiting dilution assay and analyzed for cathepsin X expression with quantitative real time PCR analysis, quantitative ELISA and active site labeling of cathepsin X.

Cytoplasmic and organelle dyes. T cells were labeled with 2.5 μM carboxyfluorescein succinimidyl ester (CFSE), 5 μg/ml Hoechst, 200 nM Mitotracker, 100 nM LysoTracker (all purchased from Molecular Probes) according to the manufacturer's protocol.

Specific cathepsin X inhibitors. Neutralizing mouse monoclonal antibody (mAb) against cathepsin X (2F12) was prepared from mouse hybridoma cell line as described [11], and used at a concentration of 1 μM. Cathepsin X-specific epoxysuccinyl-based inhibitor AMS36 [12] was used at a concentration of 3 μM.

Live-cell imaging. Eight-well chambered coverglasses (LabTek Chambered Borosilicate Coverglass, Nalge Nunc International) were precoated with 50 μL 100% Matrigel (BD Biosciences, USA) and allowed to solidify for 20 min at 37°C. Jurkat T lymphocytes were seeded onto Matrigel as a single-cell suspension (5×10^4 cell/ml) in complete medium containing 2% Matrigel. Cells were allowed to settle for 24 h at 37°C with 5% CO_2. They were tracked at 1.5–2.5-min intervals for 4–16 h at 37°C, 5% CO_2. Phorbol 12-myristate 13-acetate (PMA, 50 nM; Sigma) was used for Jurkat T cell activation. To investigate the effect of ROCK inhibitor and the highly specific inhibitor of class II myosin ATPase activity, Jurkat T cells were incubated with 20 μM Y-27632 (Sigma) and 50 μM blebbistatin (Sigma), respectively, in the presence of 20 mM Mg^{2+} for 24 h. To induce F-actin depolymerization in inhibition studies, 10 μM cytochalasin D was added. Images were taken using an Olympus IX 81 motorized inverted microscope and CellR software. Brightness and contrast were changed in some images only to increase visibility of nanotubes.

For imaging GFP-conjugated proteins, pcDNA3-α-actinin-GFP (Addgene) or pcDNA3-cathepsin X-GFP was transiently transfected in Jurkat cells. pcDNA3-cathepsin X-GFP was prepared using the CT-GFP fusion expression kit (Invitrogen). Images were taken using an Olympus IX 81 motorized inverted microscope and CellR software.

For FRET measurements, pcDNA3-α_L-CFP and pcDNA3-β_2-mYFP provided by Dr. Tim Springer (Addgene) were transiently transfected in Jurkat cells. A Zeiss LSM 510 META spectral imaging system was used to image cells expressing the two vectors. CFP or YFP were laser excited at 458 or 514 nm for determining the FRET effect or transfection efficiency, respectively.

Fixing and immunostaining Jurkat cells. Jurkat T cells were stained as described previously [6]. Actin was labeled with phalloidin-tetramethylrhodamine B isothiocyanate conjugate (Fluka) (500 ng/ml). Cathepsin X was labeled with Alexa Fluor 488 (Molecular Probes) labeled mouse 2F12 mAb (10 μg/ml), which recognizes the mature form. For labeling integrin, talin or tubulin, the primary antibodies were goat anti-human integrin LFA-1 N-18, goat anti-human talin or

anti-β tubulin H-235-AF488 (5 μg/ml) from Santa Cruz Biotechnology. Primary antibody mAb 24, provided by Dr. Nancy Hogg (Macrophage Laboratory, Imperial Cancer Research Fund, Lincoln's Inn Fields, London, UK) was used to label active LFA-1. Fluorescence microscopy was performed using a Carl Zeiss LSM 510 confocal microscope. Alexa Fluor 488 and Alexa 633 were excited with an argon (488 nm) or He/Ne (543 nm) laser, and emission was filtered using a narrow band LP 505–530 nm (green fluorescence) or 560 nm (red fluorescence) filter, respectively. Images were analyzed using Carl Zeiss LSM image software 3.0.

Flow cytometric analysis. Comparative analysis of transfer of mitochondria or CFSE dye in cells after 24 h of co-cultivation in Matrigel was performed on a FACSCalibur (Becton Dickinson). For labeling of mitochondria, cathepsin X-upregulated Jurkat cells were cultured with 200 nM Mitotracker for 40 min. Cells were then washed twice with PBS, pH 7.4. For labeling with CFSE, cells were cultured with 2.5 μM CFSE in PBS. Fresh medium was then added, and cells were placed on ice for 10 min and then washed twice with PBS, pH 7.4. Unlabeled and labeled cells were seeded onto Matrigel in 1:1 ratio and co-cultured for 24 h at 37°C with 5% CO_2. Excitation laser (488 nm) was used to detect Mitotracker and CFSE. The detector/amplifier setup was as follows: FSC: E-1, 5.71, Lin; SSC 332, Lin; FL1: 450, Log, FL2: 450, Log.

Statistical analysis

SPSS PC software (Release 13.0) was used for statistical analysis for all data. The difference between the groups was evaluated using the non-parametric Mann-Whitney test. p values of <0.05 were considered to be statistically significant. Error bars are shown as SD, unless stated otherwise.

Results and discussion

Nanotube formation in cathepsin X-upregulated Jurkat T cells. Cathepsin X-upregulated Jurkat T cells were compared to wild type Jurkat T cells by characterizing phenotypic changes in cells cultured on either Matrigel (Fig. 1A) or intercellular adhesion molecule 1 (ICAM-1)-coated surfaces (Fig. 1B) and imaging by live microscopy. After 24 h, of cathepsin X-upregulated Jurkat T cells (n=350), 28% underwent spontaneous shape polarization and developed uropods (Fig. 1C), in contrast to wild-type Jurkat cells (n=455), of which only 2% spontaneously formed polarized morphology (Fig. 1D). The uropod is a distinctive morphological and functional region projecting at the trailing edge of the cell, formed by polar redistribution of cell surface receptors and cytoskeletal elements [13]. It serves as a force-driven protrusion in T lymphocyte migration [13]. The uropods of cathepsin X-upregulated Jurkat T cells finally elongated to nanotubes and formed cell-to-cell connections (Fig. 1E and F, and Videos 1–3). Typically, a bulbous tip (Fig. 1G) was present at the end of the nanotube arising from extended uropod. This represents a remnant of the uropod and functions as a refined sensory mechanism (Video 4) capable of binding tightly to the connected cell. Of the cathepsin X-upregulated Jurkat T cells (n>350), after 24-h incubation, 20% were connected by nanotubes (Fig. 1C and H), representing 67% of uropod-forming cells (Fig. 1H). Once formed, the nanotube-interconnection arising from extended uropods persisted for several hours (Videos 2 and 5), whereas intercellular contact-provoked nanotubes, formed by Jurkat T cells coming into contact and then moving apart, decayed much more rapidly (within 1 h) (Fig. 1I and J, and Video 6). Intercellular contact-provoked nanotubes were substratum independent and hovered in 2% Matrigel, providing an effective support. Nanotubes arising from the extended uropod were, at least in the uropod-emanating phase, substratum dependent; however, once formed, the tip of the uropods and the nanotubes extending from the uropods exhibited contact independence and were able to move around and connect with other cells (Fig. 1B and Video 3). Albeit rarely, nanotubes could be interconnected (Fig. 1K) or branched, such that one cell formed multiple nanotubes simultaneously (Fig. 1L). PMA induced similar uropods and nanotube connections in T lymphocytes (23%, n=470) (Fig. S1A). In cathepsin X-upregulated Jurkat cells, the effect of PMA was apparently additive (Fig. S1B and 1H); the percentage of connected T cells reached 36% (n=550), representing 89% of uropod-forming cells. The specific inhibitor AMS36 (Fig. S1C) and the neutralizing mAb 2F12 (Fig. 1M) against cathepsin X both prevented uropod elongation and nanotube outgrowth [5% (n=430) and 3% (n=360) of nanotube connected cells, respectively].

The uropod extension and nanotube formation induced by cathepsin X resemble that caused by other factors that activate LFA-1. Activation of LFA-1 integrin receptor triggers intracellular signaling, thereby activating RhoA-ROCK signaling pathway and myosin heavy chain IIA recruitment, resulting finally in de-adhesion of the trailing edge, in contrast to the role of LFA-1 activation at the leading edge. This is consistent with the proteolytic function of

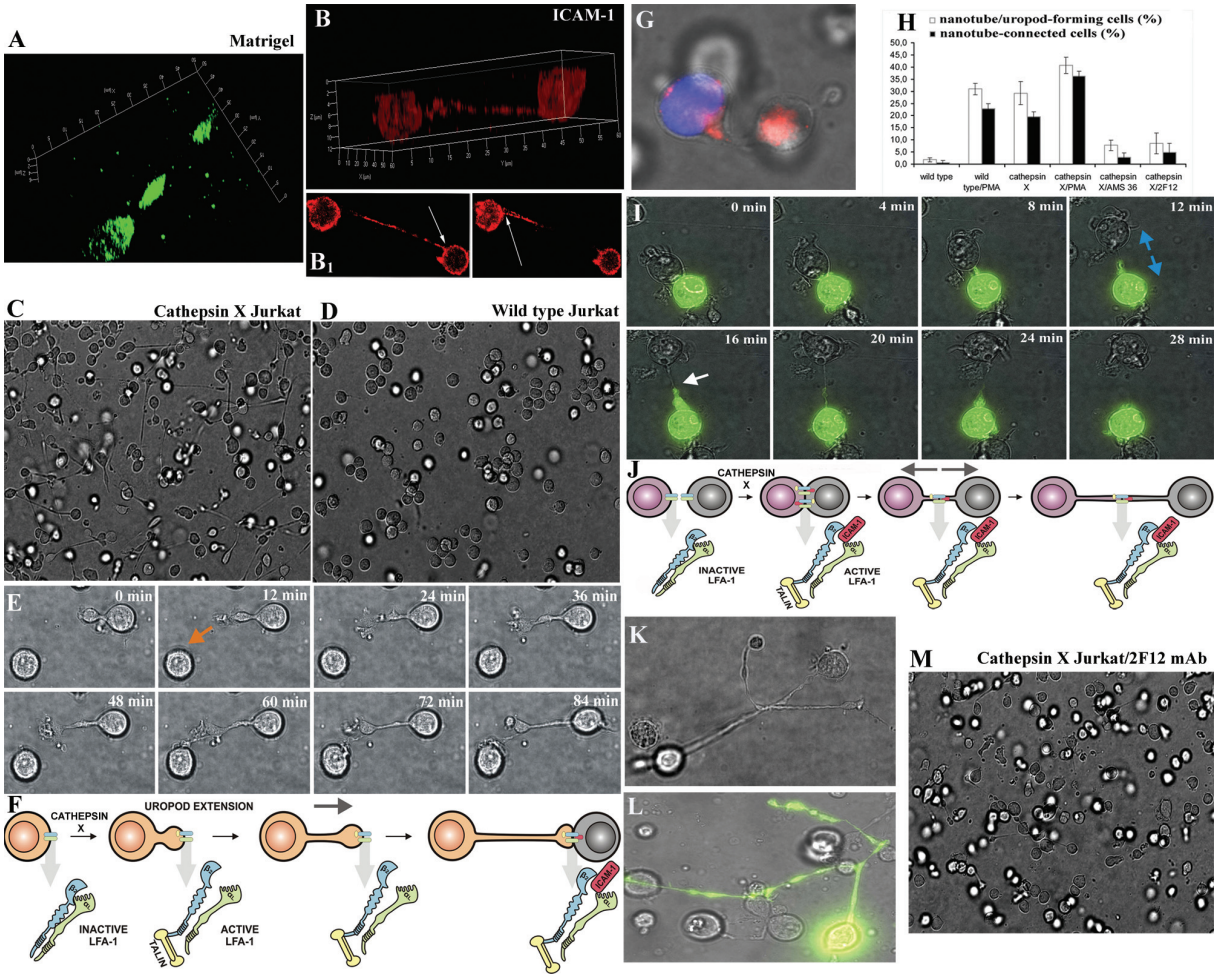

Figure 1. Cathepsin X-upregulated Jurkat T cells in a three-dimensional environment exhibit an extreme uropod extension and nanotube outgrowth. (*A, B*) Three-dimensional reconstruction of cathepsin X (*A*) or active LFA-1 detected with mAb 24 (*B*) in cathepsin X-upregulated Jurkat T cells cultured on Matrigel (*A*) or ICAM-1 (*B*). The figure shows that the uropod-extended nanotube does not lie on the substratum. (B_1) Two confocal images along the Z-direction demonstrate the connection between the two cells. (*C*) In transfected cells (n=350) cathepsin X induced the formation of a polarized phenotype with extreme uropod elongation, finally leading to cell contact formation. (*D*) Wild-type Jurkat T cells (n=455) remained in a spherical shape after 24 h of incubation in Matrigel. (E, F, I, J) LFA-1 activation is responsible for two distinct pathways of nanotube formation in Jurkat T cells. (*E*) Time-lapse microscopy of cathepsin X-upregulated Jurkat T cells cultured in Matrigel (three-dimensional matrix) reveals that nanotubes formed upon uropod elongation in the absence of prior intercellular contact. The extended uropod develops highly motile lamellipodia-like cell protrusions at its end and is subsequently elongated towards a neighboring cell until it makes contact with it. The connection persists for several minutes up to hours (Video 3). (*F*) The proposed mechanism of uropod extension and nanotube outgrowth *via* cathepsin X-mediated persistent LFA-1 activation. Whereas the ICAM-1 counter-molecule binds to the extracellular domain, talin binds to the cytoplasmic tail of LFA-1, enabling inside-out driven actin reorganization, uropod formation and its extreme elongation. This results in intercellular nanotubular contact formation. (*G*) Cathepsin X-upregulated Jurkat cells were labeled with Mitotracker and Hoechst. Although occasionally very similar in morphology, the bulbous tip of the uropod can be distinguished from the cell body as it does not contain nucleus labeled with Hoechst. (*H*) Uropod extension and nanotube outgrowth were estimated in wild-type and cathepsin X-upregulated Jurkat T cells, activated or not with phorbol myristate acetate (PMA) or treated with cathepsin X inhibitors. Inhibition of cathepsin X with either AMS36 (3.8-fold; $p<0.001$) or 2F12 mAb (3.4-fold; $p<0.001$) decreased uropod extension. PMA increased uropod extension in wild-type and cathepsin X-upregulated Jurkat T cells (5.3-fold and 3.7-fold, respectively; $p<0.001$). (*I*) Consecutive video sequences of cathepsin X-upregulated Jurkat T cells showing nanotube formation following intercellular contact (Video 6). The nanotube is not an open-ended tunnel but is separated by a distinct junction between two cells. This is evident since only one of the cells expresses α-actinin tagged with GFP. (*J*) Proposed mechanism of nanotube formation following homotypic T cell contact formation. LFA-1/ICAM-1 interactions arising in T cell aggregation are increasingly formed in cathepsin X-upregulated Jurkat cells. Homotypic T cell aggregation results from or precedes LFA-1 receptor activation. Prolonged LFA-1 activation enables cytoskeletal reorganization, similar to that associated with uropod outgrowth, with talin binding to cytoplasmic tail of the β_2 subunit and subsequent membrane nanotube formation as cells depart. (*K*) Nanotubes are occasionally seen to interconnect more than two cells. (*L*) Cathepsin X-upregulated-Jurkat T cells expressing GFP-tagged actinin demonstrate the branched morphology of nanotubes formed in Matrigel. (*M*) Cathepsin X-neutralizing mAb 2F12 (n=430) significantly inhibited Jurkat T cell polarization and nanotube formation.

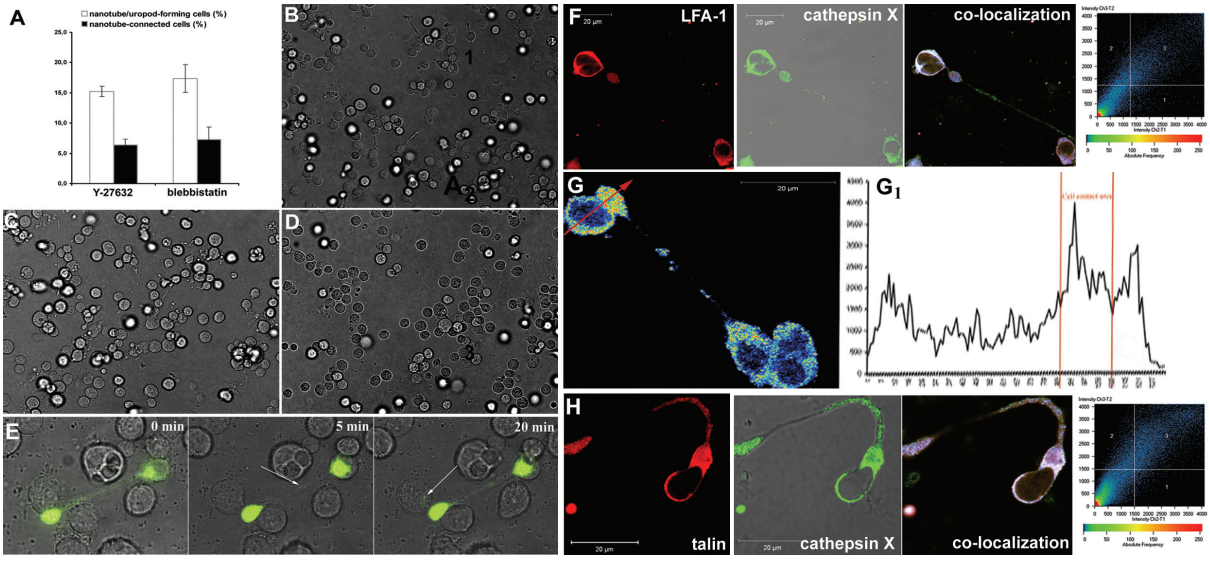

Figure 2. LFA-1 receptor activation in nanotube formation. (*A–D*) Effect of inhibiting ROCK and class II myosin ATPase activity on uropod extension and nanotube outgrowth in wild-type Jurkat T cells upon incubation in Matrigel. (A) Uropod extension and nanotube outgrowth were estimated in wild type Jurkat T cells, activated or not with Mg^{2+} and treated with ROCK inhibitor Y-27632 or highly specific inhibitor of class II myosin ATPase activity, blebbistatin. Y-27632 and blebbistatin, respectively, increased uropod extension in wild-type Jurkat T cells (15.23% and 17.38%, respectively; $p<0.001$) resulting in nanotubular intercellular connection [42.71% (Y27632) and 41.30% (blebbistatin) of uropod extending cells, respectively; $p<0.001$]. (*B–D*) Phase images of Mg^{2+}-stimulated Jurkat T cells after 24-h incubation in the presence of blebbistatin (*B*), 20 μM Y-27632 (*C*) or in the absence of inhibitors (*D*). (*E*) Time-lapse microscopy of wild-type Jurkat T cells transiently transfected with cathepsin X tagged with GFP reveals transport of cathepsin X-containing vesicles (lysosomes) along nanotubes (arrows). After 20 min, cathepsin X-GFP could be traced in the nanotube-connected cell not transfected with cathepsin X-GFP. (*G*) Localization of active LFA-1 (mAb 24) is shown with range indicator profile and is particularly evident in the uropod bulge at the cell contact region of cathepsin X-upregulated Jurkat T cells (G_1). (*F, H*) In co-localization experiments fluorescent dyes (cathepsin X, Alexa 488: green fluorescence; LFA-1 (*F*) and talin (*H*), Alexa 633: red fluorescence) were imaged sequentially in a line-interlace mode to eliminate cross-talk between the channels. Threshold value was determined arbitrarily and set to 30% of the maximal brightness level. The mask of the pixels above the threshold in both channels (blue color) and the contour plot are shown for images demonstrating high co-localization of cathepsin X and LFA-1 (*F*) or talin (*H*). Co-localization of talin or LFA-1 with cathepsin X as well as cathepsin X localization (*E*) is particularly evident on the membrane of the cell in the uropod outgrowing area and in the bulbous tip of the uropod.

lysosomes in this region [14]. However, constant activation of LFA-1 integrin receptor results in insufficient retraction force, uropod extension and nanotube outgrowth. Blebbistatin, a noncompetitive myosin II inhibitor, prevents non-muscle myosin heavy chain IIA recruitment to LFA-1, resulting in its activation at the uropod, with consequent extreme uropod elongation (17.38%, n=280) (Fig. 2A and B, [5]) and nanotube outgrowth (41.3% of uropod-forming cells). Gurke et al. [15] also demonstrated a strong induction of the number of nanotubes and organelle transfer by blebbistatin. Inhibition of Rho kinase/ROCK in human T lymphocytes resulted in similar uropod elongation (15.23%, n=413) (Fig. 2A and C, [16]) and nanotube outgrowth (42.71% of uropod-forming cells). Further, the RhoA-ROCK pathway may impinge on myosin heavy chain IIA to regulate LFA-1 adhesion [16]. Thus, persistent LFA-1 activation (due to cathepsin X overexpression or inhibition of RhoA-ROCK pathway or myosin heavy chain IIA recruitment) results in extreme uropod elongation.

Mechanism of LFA-1 integrin activation by cathepsin X. Cathepsin X similarly induces persistent LFA-1 activation in Jurkat T cells, which we propose is a mechanism of uropod elongation and nanotube outgrowth. Although cathepsin X belongs to a class of cysteine cathepsins, it localizes in the perimembrane region. The exact mechanism of cathepsin X translocation, in particular whether cathepsin X translocation takes place after lysosomal translocation to the plasma membrane, is being intensively studied. Lysosomes have been shown to translocate to the plasma membrane upon different activation stimuli, and recently Sloane et al. [17] have shown that cathepsin B participates in podosome-mediated extracellular matrix degradation. In our previous study [10], we have shown that cathepsin X affects the biogenesis of podosomes by regulating integrin activity.

LFA-1 binds to cytoskeletal and regulatory proteins, controlling integrin signaling to the cytoskeleton. In uropod-extending Jurkat T cells, cathepsin X was localized on the membrane in the uropod outgrowing

zone as well as on the membrane of the bulbous tip formed by the uropod (Figs. 1A and 2E). The strong co-localization of cathepsin X with LFA-1 at the tip of extended uropods (Fig. 2F) in Jurkat T cells supports its role in LFA-1 regulation at the growing end of the uropod. LFA-1 is normally present in uropods in its inactive form [18]; however, in cathepsin X-upregulated Jurkat T cells, LFA-1 is shown to be active by detection with mAb 24. This mAb recognizes the open, high-affinity form of the integrin [19] in the bulbous tip of the uropod, especially at its point of contact with the connected cell (Fig. 2G and G_1). LFA-1 acts as a true signaling receptor, causing cytoskeletal reorganization. Talin, a major cytoskeletal actin-binding protein, binds to the integrin β_2 tail and plays a critical role in integrin activation [20]. Talin strongly co-localized with cathepsin X (Fig. 2H). In agreement with these observations, uropod elongation and subsequent nanotube formation on cathepsin X-upregulated Jurkat cells is mediated by permanently activated LFA-1 [7], which binds talin in this activated conformation. Similarly, ligation of cell surface receptors, such as T cell receptor, or chemokine receptors, as well as treatment with phorbol esters also promotes LFA-1 activation [21], explaining the resulting morphological changes similar to those in cathepsin X-upregulated Jurkat T cells (Fig. S1A).

One striking feature that has been reported for nanotubes formed by immune cells (T cells [22] and NK cells [23, 24]) is that nanotube formation is cell contact dependent, whereas in other cell types (neuronal cells [1], fibroblast and epithelial cells [25, 26]) their formation is driven by actin protrusion. The reasonable explanation for this is that non-activated primary T lymphocytes, specifically, are devoid of cell extensions (filopodia, lamellipodia, uropods, etc.) and require stimulus from a chemoattractant such as chemokine to attach to integrin ligands. However, for preactivated T lymphoblasts, LFA-1-mediated binding to an ICAM-1-expressing surface is sufficient to cause cell polarization and migration without the involvement of chemokines [5, 27]. A FRET study of non-activated and PMA-activated Jurkat cells cultured on Matrigel and transfected with α_L-CFP and β_2-YFP demonstrated this difference in LFA-1 activity (Fig. 3A). Whereas, in the control/α_L-CFP+β_2-YFP Jurkat T cells, LFA-1 is not constitutively active (Fig. 3B), LFA-1 of the PMA/α_L-CFP+β_2-YFP Jurkat cells is active on the cell surface in the nanotubes formed from the extended uropods (Fig. 3C) as well as in cell contact-triggered nanotubes (Fig. 3D). LFA-1-mediated signaling cascades induce actin reorganization, enabling T cell polarization. The actin-depolymerizing drug cytochalasin D significantly reduced uropod elongation and nanotube formation in cathepsin X-upregulated Jurkat cells (Fig. 3E). Similarly, lactrunculin B abolished nanotube formation in PC12 pheocromocytoma cells [1]. Thus, our results show that actin reorganization, mediated by LFA-1 activation, is critical for effective uropod formation and nanotube outgrowth. Live microscopy of cathepsin X-upregulated Jurkat cells in a three-dimensional environment confirms that the uropod extension and nanotube outgrowth are not cell contact dependent, but are driven by cytoskeletal reorganization (Videos 1–3); a three-dimensional environment provides support for nanotubes to grow very long, with a curved morphology (Figs. 1L and 2H). On the other hand, nanotube formation provoked by intercellular contact (Fig. 1I and J and Video 6) may also depend on LFA-1 activation, triggered by cell contact ICAM-1/LFA-1 interaction, explaining the time dependence for T cell nanotube formation after cell separation [22]. Namely, T cell homotypic intercellular connections formed *via* LFA-1/ICAM-1 connections are also increasingly formed in cathepsin X-upregulated Jurkat T cells [6]. In this way, LFA-1 activation is responsible for two distinct pathways of nanotube formation in Jurkat T cells (Fig. 1F and J).

Structure of nanotubes formed by cathepsin X-upregulated Jurkat T cells. The nanotubes formed by cathepsin X-upregulated Jurkat cells in a three-dimensional environment contain tubulin as well as actin (Fig. 3F and G). Since nanotubes arise from extended uropods, this observation is not surprising. As the uropod buds out, the microtubules retract into the uropod lumen, thereby increasing T cell deformability and facilitating migration [28]. However, nanotubes formed after intercellular contact are devoid of microtubules, as they do not originate from a microtubule-containing cell extension [22]. In a striking analogy, two distinct types of nanotube connect human macrophages [23], one containing only F-actin, and the other containing microtubules as well. Macrophage microtubule-containing nanotubes are thicker, with a bulbous tip at one end, and closely resemble cathepsin X-upregulated Jurkat nanotubes formed in a three-dimensional environment, in contrast to the thin, actin-containing nanotubes formed after intercellular contact. We propose that in monocytes and macrophages, nanotubes containing actin and microtubules derive from microtubule-containing cell protrusions, such as RhoA-ROCK-regulated lamellipodia [29], whereas nanotubes containing actin but lacking microtubules derive from filopodia or after intercellular contact. In cathepsin X-upregulated Jurkat T cells thick nanotubes were prevalent and formed after uropod elongation and the intercel-

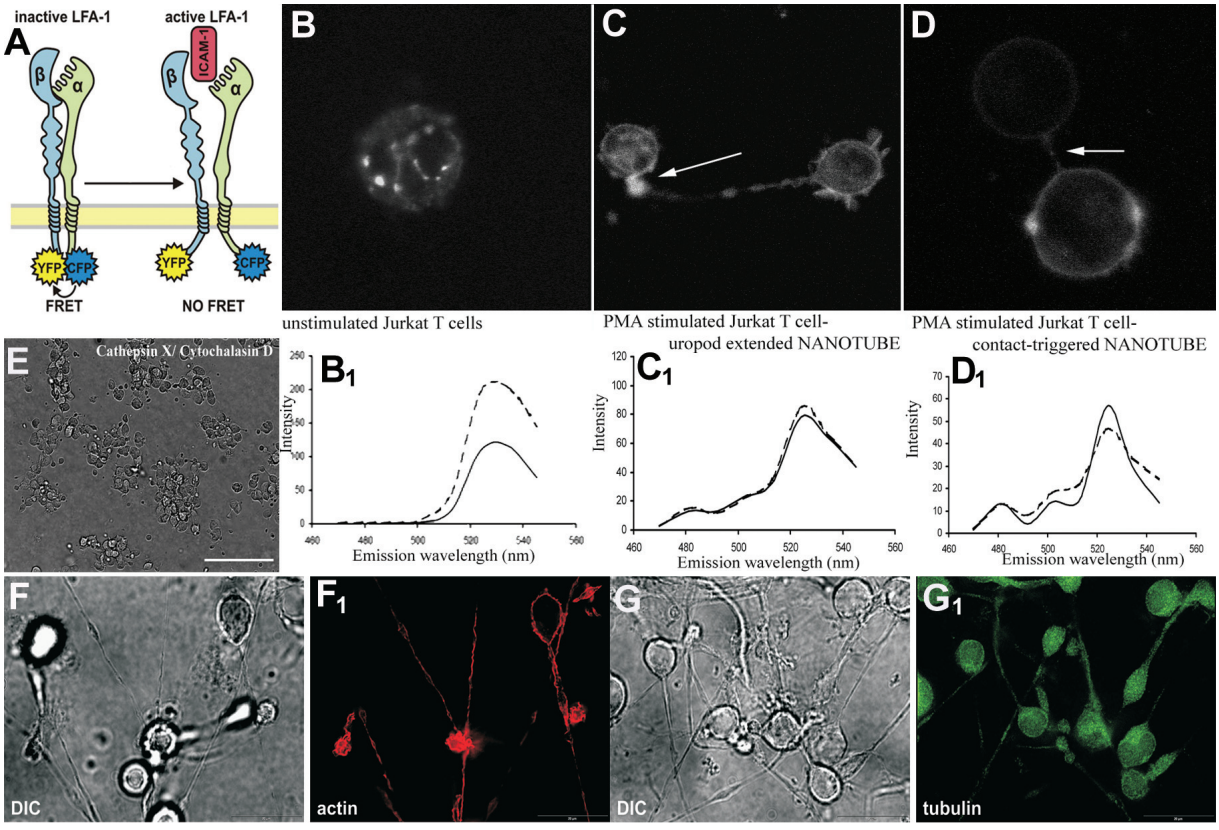

Figure 3. Cytoskeletal organization and integrin LFA-1 ($\alpha_L\beta_2$) activation. (*B–D*) A Zeiss LSM 510 META spectral imaging system was used to image FRET effect in non-activated (*B*) and PMA-activated (*C, D*) Jurkat T cells transfected with pcDNA3/α_L-mCFP and β_2-mYFP and cultured in medium (*B*) or in Matrigel (*C, D*). The emission spectrum of α_L-mCFP and β_2-mYFP in non-stimulated Jurkat T cells (B_1) shows peak emission at 525 nm, indicating the fluorescence transfer from CFP to YFP characteristic of non-activated LFA-1 (*A*). PMA-activated Jurkat T cells forming extended uropod- (C_1) or intercellular contact-driven nanotubes (D_1) demonstrate CFP emission spectrum, indicating absence of FRET and increase in LFA-1 activation (*A*). The statistical analysis of fluorescence transfer was also done. The mean ratio of YFP (483 nm) to CFP (526 nm) emission [determined in 20 randomly selected circular regions of interest (diameter 15 pixels)] is 20.57±8.97 in non-activated Jurkat T cells, which differs significantly from 2.40±0.80 in PMA activated Jurkat T cells ($p<0.001$). (*E*) After treatment of cathepsin X-upregulated Jurkat cells with cytochalasin D, an F-actin depolymerizing substance, no nanotubes were detected. (*F, G*) Differential interference contrast and phalloidin (F_1) or anti-β tubulin (G_1) staining of nanotubes formed after extreme uropod elongation in cathepsin X-upregulated Jurkat T cells demonstrate the presence of actin and tubulin inside the nanotubes.

lular contact-provoked nanotubes were thin. Whereas the thick nanotubes connecting cathepsin X-upregulated Jurkat cells are seen to form a typical bulge at the end of the nanotube, thin nanotubes from each T cell define a specific junction [22], demonstrating that the membrane between Jurkat cells is not seamlessly connected between nanotubes. The latter is clearly shown for cathepsin X-upregulated Jurkat T cells transfected with α-actinin conjugated to GFP, which are connected to non-transfected Jurkat cells that are separated by a specific junction through which α-actinin could not protrude (Fig. 1I).

Nanotubular vesicular transfer in cathepsin X-upregulated Jurkat T cells. Nevertheless, nanotubes of cathepsin X-upregulated Jurkat cells can readily transfer cellular organelles. Larger organelles, such as mitochondria, labeled with Mitotracker (Fig. 4A), and lysosomes, labeled with Lysotracker (Fig. 4B and Video 7), were observed trafficking inside nanotubes, ending up within the cytoplasm of the nanotube-forming cell. Individual vesicles moved in each direction in a stepwise manner inside the nanotubes (Fig. 4C). Also, fluorescence microscopy revealed that lysosomal cathepsin X conjugated to GFP constitutively expressed in Jurkat T cells could be transferred to a connected cell *via* nanotubes (Fig. 2E). In addition, mitochondria originating from one cathepsin X-upregulated Jurkat cell can be transferred into another Jurkat cell (Fig. 4D). Mitochondria were abundant in the bulbous tip of uropods and could continuously transfer into the cytoplasm of the connected cell (Fig. 4E). This enabled efficient transfer of mitochondria between cathepsin X-upregulated Jurkat T cells in Matrigel (Fig. 4F and Video S8). On the other hand, the small cytoplasmic dye CFSE was not transferred between cells (Fig. 4G and H), although it entered the nanotubes (Fig. 4G). Clearly, cell-to-cell

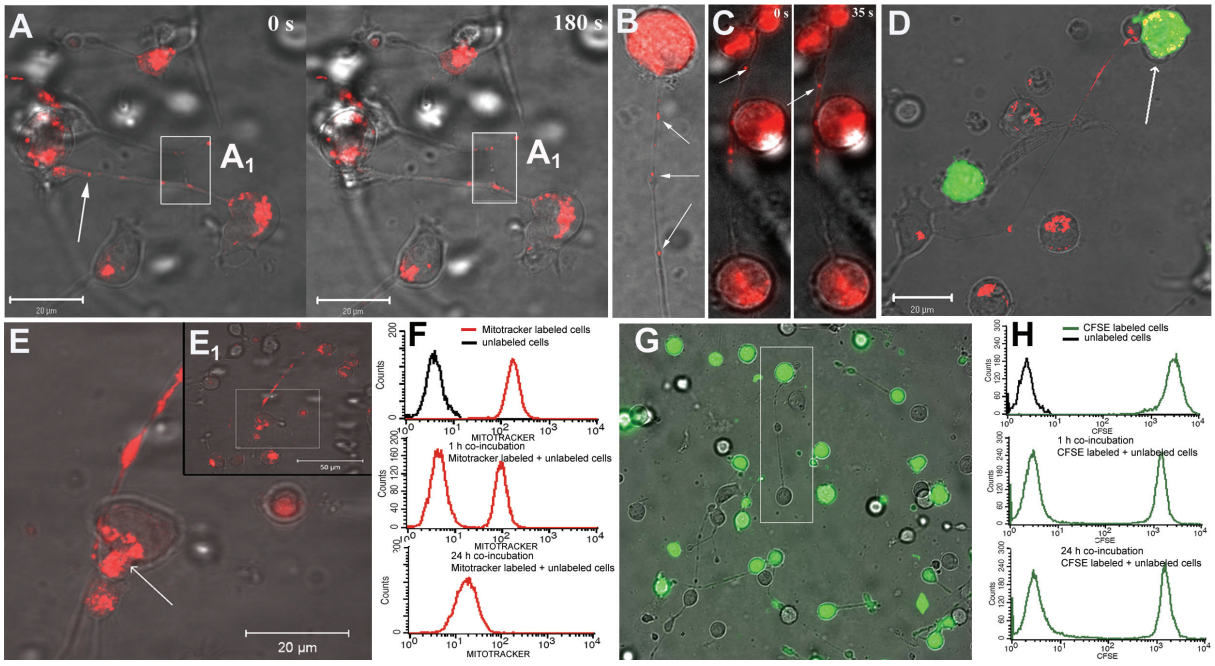

Figure 4. Nanotube-based intercellular organelle transport in cathepsin X-upregulated Jurkat T cells. (*A*) Consecutive images of Mitotracker-labeled cathepsin X-upregulated Jurkat T cells. The inset (A_1) depicts a thin nanotube connecting separate large nanotubes. Mitochondria were not observed inside this thin nanotube interconnection. The arrow indicates mitochondria trafficking inside a large nanotube. (*B*) Arrows indicate lysosomes marked with Lysotracker inside a nanotube of a cathepsin X-upregulated Jurkat cell. (*C*) A selected frame of a video sequence (Video 7) showing Lysotracker-labeled organelle movement within a nanotube. (*D*) Cathepsin X-upregulated Jurkat cells stained with CFSE were mixed with Mitotracker-labeled cells, co-cultured for 24 h and analyzed by confocal microscopy. Arrow indicates a CFSE-labeled cell that received mitochondria from a Mitotracker-labeled cell *via* a nanotube. A neighboring CFSE-labeled cell is devoid of Mitotracker-labeled mitochondria. (*E*) Confocal image of Mitotracker-labeled cathepsin X-upregulated Jurkat cells in Matrigel shows a strong passage of mitochondria through the cellular junction at the bulbous tip of the nanotube (Video 8). The inset (E_1) shows a reduced view of the nanotube connection. (*F, H*) Flow cytometric analysis of cathepsin X-upregulated Jurkat co-cultures of unlabelled and Mitotracker-labeled (*F*) or CFSE-labeled (*H*) cells. Whereas mitochondria are readily transferred (*F*), CFSE is not transferred between cells (*G, H*), although it can enter the nanotubes (*G*).

transfer of vesicles is preferred by nanotubes. The process may be mediated by clathrin since electron micrographs reveal the tip of a nanotube interacting with clathrin-coated pits of the other connected Jurkat cell [22]. In accordance with this hypothesis, Rho/ROCK and myosin II, which regulate LFA-1 activity, also induce polarized distribution of clathrin structures at the uropod and their endocytic ability [30]. Nevertheless, the precise mechanism of cell organelle transfer by nanotubes remains to be elucidated.

In conclusion, activation of LFA-1 integrin receptor by cathepsin X has been identified as a mechanism of membrane nanotube formation in T lymphocytes. Cathepsin X activates LFA-1 and promotes massive uropod elongation and subsequent nanotube formation. This formation of nanotubes triggered by LFA-1 activation enables transfer of subcellular vesicles at the moment of cell activation, either in conjunction with T cell receptor activation or following homotypic cell interaction. This opens up the importance of nanotube-mediated transfer in T lymphocyte activation, without the need for direct contact with the antigen-presenting cell.

Acknowledgements. This work is supported by the Research Agency of the Republic of Slovenia, grant P4–0127 (J.K.), and 6th EU Framework IP project CancerDegradome (J.K.). We thank Urša Pečar Fonovič, M.Sc. for the generous gift of active recombinant cathepsin X, Dr. N. Hogg for the generous gift of mAb 24, Dr. T. Springer for kindly providing plasmid DNA constructs for α_L-mCFP and β_2-mYFP. The authors acknowledge Prof. R. Pain for critical reading of the manuscript. Author contributions: N.O. conceived the study, N.O. and Z.J. designed and performed experiments and analyzed the data, B.D. helped prepare pcDNA3-cathepsinX-GFP, N.O. wrote the paper with input from Z.J. and J.K., A.M.S. and M.B. designed and synthesized specific cathepsin X inhibitor AMS36, J.K. supervised the study. Competing financial interests: The authors declare having no competing financial interests.

1 Rustom, A., Saffrich, R., Markovic, I., Walther, P. and Gerdes, H. H. (2004) Nanotubular highways for intercellular organelle transport. Science 303, 1007–1010
2 Gerdes, H. H., Bukoreshtliev, N. V. and Barroso, J. F. (2007) Tunneling nanotubes: A new route for the exchange of components between animal cells. FEBS Lett. 581, 2194–2201
3 Zhu, D., Tan, K. S., Zhang, X., Sun, A. Y., Sun, G. Y. and Lee, J. C. (2005) Hydrogen peroxide alters membrane and cytoskeleton properties and increases intercellular connections in astrocytes. J. Cell Sci. 118, 3695–3703
4 Hynes, R. O. (2002) Integrins: Bidirectional, allosteric signaling machines. Cell 110, 673–687

5 Morin, N. A., Oakes, P. W., Hyun, Y. M., Lee, D., Chin, E. Y., King, M. R., Springer, T. A., Shimaoka, M., Tang, J. X., Reichner, J. S. and Kim, M. (2008) Nonmuscle myosin heavy chain IIA mediates integrin LFA-1 de-adhesion during T lymphocyte migration. J. Exp. Med. 205, 195–205
6 Jevnikar, Z., Obermajer, N., Bogyo, M. and Kos, J. (2008) The role of cathepsin X in the migration and invasiveness of T lymphocytes. J. Cell Sci. 121, 2652–2661
7 Obermajer, N., Repnik, U., Jevnikar, Z., Turk, B., Kreft, M. and Kos, J. (2008) Cysteine protease cathepsin X modulates immune response via activation of beta-2 integrins. Immunology 124, 76–88
8 Victor, B. C. and Sloane, B. F. (2007) Cysteine cathepsin non-inhibitory binding partners: Modulating intracellular trafficking and function. Biol. Chem. 388, 1131–1140
9 Obermajer, N., Premzl, A., Zavasnik-Bergant, T., Turk, B. and Kos, J. (2006) Carboxypeptidase cathepsin X mediates beta2-integrin-dependent adhesion of differentiated U-937 cells. Exp. Cell Res. 312, 2515–2527
10 Obermajer, N., Švajger, U., Bogyo, M., Jeras, M. and Kos, J. (2008) Maturation of dendritic cells depends on proteolytic cleavage by cathepsin X. J. Leukoc. Biol. 84, 1306–1315
11 Kos, J., Sekirnik, A., Premzl, A., Zavasnik-Bergant, V., Langerholc, T., Turk, B., Werle, B., Golouh, R., Repnik, U., Jeras, M. and Turk, V. (2005) Carboxypeptidases cathepsins X and B display distinct protein profile in human cells and tissues. Exp. Cell Res. 306, 103–113
12 Sadaghiani, A. M., Verhelst, S. H. L., Gocheva, V., Hill, K., Majerova, E., Stinson, S., Joyce, J. A. and Bogyo, M. (2007) Potency and selectivity of epoxysuccinyl-based inhibitors of papain-family cysteine proteases. Chem. Biol. 14, 499–511
13 Vicente-Manzanares, M. and Sanchez-Madrid, F. (2004) Role of the cytoskeleton during leukocyte responses. Nat. Rev. Immunol. 4, 110–122
14 Mohamed, M. M. and Sloane, B. F. (2006) Cysteine cathepsins: Multifunctional enzymes in cancer. Nat. Rev. Cancer 6, 764–775
15 Gurke, S., Barroso, J. F. V., Hodneland, E., Bukoreshtliev, N. V., Schlicker, O. and Gerdes, H. H. (2008) Tunneling nanotube (TNT)-like structures facilitate a constitutive, actomyosin-dependent exchange of endocytic organelles between normal rat kidney cells. Exp. Cell Res. 314, 3669–3683
16 Smith, A., Bracke, M., Leitinger, B., Porter, J. C. and Hogg, N. (2003) LFA-1-induced T cell migration on ICAM-1 involves regulation of MLCK-mediated attachment and ROCK-dependent detachment. J. Cell Sci. 116, 3123–3133
17 Tu, C., Ortega-Cava, C. F., Chen, G., Fernandes, N. D., Cavallo-Medved, D., Sloane, B. F., Band, V. and Band, H. (2008) Lysosomal cathepsin B participates in the podosome-mediated extracellular matrix degradation and invasion via secreted lysosomes in v-Src fibroblasts. Cancer Res. 68, 9147–9156
18 Smith, A., Carrasco, Y. R., Stanley, P., Kieffer, N., Batista, F. D. and Hogg, N. (2005) A talin-dependent LFA-1 focal zone is formed by rapidly migrating T lymphocytes. J. Cell Biol. 170, 141–151
19 Alonso, J. L., Essafi, M., Xiong, J. P., Stehle, T. and Arnaout, M. A. (2002) Does the integrin alphaA domain act as a ligand for its betaA domain? Curr. Biol. 12, R340–R342
20 Tadokoro, S., Shattil, S. J., Eto, K., Tai, V., Liddington, R. C., de Pereda, J. M., Ginsberg, M. H. and Calderwood, D. A. (2003) Talin binding to integrin beta tails: A final common step in integrin activation. Science 302, 103–106
21 Stewart, M. P., McDowall, A. and Hogg, N. (1998) LFA-1-mediated adhesion is regulated by cytoskeletal restraint and by a Ca^{2+}-dependent protease, calpain. J. Cell Biol. 140, 699–707
22 Sowinski, S., Jolly, C., Berninghausen, O., Purbhoo, M. A., Chauveau, A., Köhler, K., Oddos, S., Eissmann, P., Brodsky, F. M., Hopkins, C., Onfelt, B., Sattentau, Q. and Davis, D. M. (2008) Membrane nanotubes physically connect T cells over long distances presenting a novel route for HIV-1 transmission. Nat. Cell Biol. 10, 211–219
23 Onfelt, B., Nedvetzki, S., Benninger, R. K., Purbhoo, M. A., Sowinski, S., Hume, A. N., Seabra, M. C., Neil, M. A., French, P. M. and Davis, D. M. (2006) Structurally distinct membrane nanotubes between human macrophages support long-distance vesicular traffic or surfing of bacteria. J. Immunol. 177, 8476–8483
24 Roda-Navarro, P. and Reyburn, H. T. (2007) Intercellular protein transfer at the NK cell immune synapse: Mechanisms and physiological significance. FASEB J. 21, 1636–1646
25 Sherer, N. M., Lehmann, M. J., Jimenez-Soto, L. F., Horensavitz, C., Pypaert, M. and Mothes, W. (2007) Retroviruses can establish filopodial bridges for efficient cell-to-cell transmission. Nat. Cell Biol. 9, 310–315
26 Lehmann, M. J., Sherer, N. M., Marks, C. B., Pypaert, M. and Mothes, W. (2005) Actin- and myosin-driven movement of viruses along filopodia precedes their entry into cells. J. Cell Biol. 170, 317–25
27 Dustin, M. L., Bromley, S. K., Kan, Z., Peterson, D. A. and Unanue, E. R. (1997) Antigen receptor engagement delivers a stop signal to migrating T lymphocytes. Proc. Natl. Acad. Sci. USA 94, 909–3913
28 Ratner, S., Sherrod, W. S. and Lichlyter, D. (1997) Microtubule retraction into the uropod and its role in T cell polarization and motility. J. Immunol. 159, 1063–1067
29 Worhylake, R. A. and Burridge, K. (2003) RhoA and ROCK promote migration by limiting membrane protrusions. J. Biol. Chem. 278, 13578–13584
30 Samaniego, R., Sanchez-Martin, L., Estecha, A. and Sanchez-Mateos, P. (2007) Rho/ROCK and myosin II control the polarized distribution of endocytic clathrin structures at the uropod of moving T lymphocytes. J Cell Sci. 120, 3534–3543